THE JOURNAL OF BIOLOGICAL CHEMISTRY VOL. 286, NO. 26, pp. 23432–23440, July 1, 2011
Printed in the U.S.A.

Increased Axonal Mitochondrial Mobility Does Not Slow Amyotrophic Lateral Sclerosis (ALS)-like Disease in Mutant SOD1 Mice*[S]

Received for publication, March 7, 2011, and in revised form, April 24, 2011 Published, JBC Papers in Press, April 25, 2011, DOI 10.1074/jbc.M111.237818

Yi-Bing Zhu[1] **and Zu-Hang Sheng**[2]

From the Synaptic Function Section, The Porter Neuroscience Research Center, NINDS, National Institutes of Health, Bethesda, Maryland 20892-3706

Reduced axonal mitochondrial transport has been observed in major neurodegenerative diseases, including fALS patients and SOD1^{G93A} mice. However, it is unclear whether this defect plays a critical role in axonal degeneration or simply reflects sequelae of general transport alteration. Using genetic mouse models combined with time-lapse imaging of live neurons, we previously discovered that axon-targeted syntaphilin (SNPH) acts as a docking receptor specific for axonal mitochondria. Deletion of the *snph* gene in mice results in a substantially higher proportion of axonal mitochondria in the mobile state without any effect on the transport of other axonal organelles. Here we address whether increased (rescued) axonal mitochondrial mobility changes the disease course by crossing fALS-linked transgenic SOD1^{G93A} and *snph*$^{-/-}$ knock-out mice. We found that a 2-fold increase in axonal mitochondrial mobility in SOD1^{G93A}/*snph*$^{-/-}$ mice did not affect the onset of ALS-like symptoms. Both SOD1^{G93A} and SOD1^{G93A}/*snph*$^{-/-}$ mice exhibit similar weight loss, deterioration in motor function and motor neuron loss, significant gliosis, and a lifespan of 152–154 days. Thus, for the first time, our study provides genetic and pathological evidence that the impairment of mitochondrial transport seen in SOD1^{G93A} mice plays a minimal role in the rapid-onset of fALS-linked pathology.

Mitochondria are essential organelles for neuronal survival and function. Neurons require specialized mechanisms to regulate mitochondrial transport along axons and retain them in growth cones, nodes of Ranvier, and synaptic terminals, where energy production and calcium homeostasis are critical (1–5). Defects in mitochondrial transport could cause local energy depletion and toxic changes in Ca^{2+} buffering, triggering synaptic dysfunction and loss. Altered transport and distribution of axonal mitochondria has been implicated in the neurodegenerative diseases such as Alzheimer, Huntington, and Amyotrophic Lateral Sclerosis (ALS).[3] However, it has not been established whether altered mitochondrial mobility plays a critical role in axonal degeneration.

Characterization of mitochondrial transport in mature neurons from aged and disease-stage neurodegenerative disease models is an important step in understanding the cellular mechanisms of neurodegeneration. ALS is a late-onset neurodegenerative disease that causes motor neuron loss (6). Mutations in Cu/Zn superoxide dismutase (SOD) genes have been found to cause familial ALS (7). Transgenic mice expressing mutant human SOD1 are clinically and pathologically similar to human ALS patients (8), becoming paralyzed in one or more limbs because of a loss of motor neurons in the spinal cord. Several laboratories have reported altered transport of axonal mitochondria in ALS patients and SOD1^{G93A} mice, as well as neurons and motor neuron NSC34 cell lines expressing SOD1^{G93A} (9–11). The presence of dysfunctional mitochondria at distal axons could be a consequence of impaired recycling or degradation of abnormal mitochondria because of reduced mobility and altered axonal transport. To slow axonal degeneration, it is proposed that increased mitochondrial transport might aid the efficient delivery of healthy mitochondria to axons and/or the removal of damaged mitochondria from distal synapses for degradation or repair. Therefore, it is important to assess whether increased (rescued) axonal mitochondrial mobility in mutant SOD1 disease models has a beneficial impact on the pathogenesis of motor neuron degeneration.

We previously discovered that axon-targeted syntaphilin (SNPH) acts as a docking receptor specific for axonal mitochondria (12). Deleting *snph* in mice results in a substantially higher proportion of axonal mitochondria in the mobile state without any effect on the transport of other axonal organelles. In the present study, we first examine *snph*$^{-/-}$ mice and found that increased axonal mitochondrial mobility by deleting *snph* has no impact on lifespan or motor function, and *snph*$^{-/-}$ mice display no observable neurodegeneration phenotype. Second, by crossing SOD1^{G93A} and *snph*$^{-/-}$ mice we address whether increasing (rescued) mitochondrial mobility has any impact on the pathogenesis of the fALS-linked SOD1^{G93A} mouse model by comparing clinical and histological observations of SOD1^{G93A} mice to the crossed SOD1^{G93A}/*snph*$^{-/-}$ mice. To our surprise, although the crossed SOD1^{G93A}/*snph*$^{-/-}$ mice

* This work was supported, in whole or in part, by the Intramural Research Program of the NINDS, National Institutes of Health (to Z.-H. S.).

[S] The on-line version of this article (available at http://www.jbc.org) contains supplemental Movies S1–S4.

[1] Graduate student in the NIH-Shanghai Jiao-Tong University Joint Ph.D. Program in Neuroscience.

[2] To whom correspondence should be addressed. Tel.: 301-435-4596; Fax: 301-480-5763; E-mail: shengz@ninds.nih.gov.

[3] The abbreviations used are: ALS, amyotrophic lateral sclerosis; ANOVA, analysis of variance; DIV, days *in vitro*; DRG, dorsal root ganglion; GFAP, glial fibrillary acidic protein; Iba-1, ionized calcium binding adaptor molecule 1; SOD1, copper/zinc superoxide dismutase 1; SNPH, syntaphilin.

exhibit a 2-fold increase in axonal mitochondrial mobility at disease stages, there is no observable improvement in the deterioration of motor function or in disease progression and lifespan. Furthermore, immunostaining of spinal cord sections from both $SOD1^{G93A}$ and $SOD1^{G93A}$/$snph^{-/-}$ mice show similar ALS-like disease histopathology that includes motor neuron loss and gliosis. Thus, our study provides genetic, cellular, and pathological evidence that challenges the prevailing hypothesis that defective transport of axonal mitochondria contributes to rapid-onset motor neuron degeneration in this mouse model.

EXPERIMENTAL PROCEDURES

Animals and Neuronal Cultures—B6.Cg-Tg ($SOD1^{G93A}$) 1Gur/J mice were originally described by Gurney *et al.* (8) and purchased from The Jackson Laboratory. Transgenic mice carrying this $SOD1^{G93A}$ express high copy number of a G93A mutant form of human SOD1. Hemozygotes are viable and fertile and exhibit a phenotype similar to ALS in humans becoming paralyzed in one or more limbs due to loss of motor neurons from the spinal cord, and have a life span of 157.1 ± 9.3 days.[4] Transgenic mice on a mixed B6SJL genetic background were backcrossed to C57BL/6J for at least 10 generations in The Jackson Laboratory to generate this congenic strain (Stock No. 004435). This strain was crossed with C57BL/6 background $snph^{-/-}$ mice to generate $SOD1^{G93A}$/$snph^{+/-}$ heterozygous mice. These mice were then crossed with $snph^{+/-}$ mice to generate WT, $SOD1^{G93A}$, $snph^{-/-}$ and $SOD1^{G93A}$/$snph^{-/-}$ littermates. Dorsal root ganglion (DRG) neuron cultures from P120-P125 mice were dissected in Hank's buffered salt solution (HBSS), followed by digestion in 2.5 units/ml dispase II and 200 units/ml collagenase (Worthington Biochemical). Tissues were triturated in Neurobasal medium and plated on coverslips coated with 100 μg/ml poly-D-lysine and 5 μg/ml laminin (Invitrogen) supplemented with B27 (Invitrogen) and 100× Glutamax (Invitrogen). The final density of cells is 2,000 per coverslip.

Mitochondrial Mobility Studies—Time-lapse imaging was performed using a Zeiss LSM 510 META confocal microscope (Zeiss Microimaging) with a P-Apochromat 40×/1.3 oil objective. Mitochondria in DIV2 DRG neurons were labeled with 100 nM MitoTracker red CMX-Ros (Invitrogen) in Neurobasal medium for 20 s. Proximal axons were captured for time-lapse imaging in a coverglass chamber (Nalge Nunc International) with Tyrode's solution at 37 °C. Kymograghs and mobility analysis were carried out as previously described (12).

Immunocytochemistry—Mice were anesthetized by intraperitoneal injection of 100 mg/kg of ketamine (Fort Dodge) and 10 mg/kg of xylazine (Akorn Inc) and euthanized by transcardial perfusion with PBS for 5 min followed by perfusion-fixation with 4% paraformaldehyde in PBS for 5 min. The spinal cord was removed and post-fixed in 4% paraformaldehyde in PBS. The lumbar region of the spinal cord and motor axons were embedded in paraffin and sectioned at 8-μm thickness. To quantify the motor neuron number, every 13th section was sampled for a total of 30 sections for each animal. Motor neurons were stained with SMI32 (Sternberger Monoclonal/Covance) and Nissl. Only large neurons with a clear nucleus and nucleolus were counted. Astrocytes and microglia were stained by GFAP (Sigma) and Iba-1 (Wako Chemicals), respectively. Three animals were used for each genotype.

For astrocyte and microglia studies, 9 spinal cord transverse sections were randomly selected from each genotype. For microglia quantification, only cells in the lateral ventral horns that were in focus and completely within the field of view were counted. NIH Image J was used to quantify the mean densities of Iba-1 and GFAP. For astrocytes, the region of interest for cell counts (lateral ventral horn) was defined using landmarks and reference points from the mouse spinal cord (15). Motor axon transverse sections from the lumbar spinal level were co-stained with antibodies against SNPH (12) and SMI32. DIV2 DRG neurons from WT and $snph^{-/-}$ were fixed with 4% paraformaldehyde in PBS for 30 min, followed by co-staining with antibodies against SNPH and cytochrome *c* (BD Pharmingen).

Determination of Disease Onset and End Point—Disease onset and animal lifespan were defined by weight and motor function. Upon reaching 13 weeks of age, animals were weighed weekly. Onset of disease was defined as the week following peak weight based on the individual weight curve for the mouse (13). Motor performance was evaluated by weekly Rotarod testing (San Diego Instruments). Mice were placed on a rotating rod that was set to accelerate from 0 to 40 rpm over the course of 180 s. The amount of time the mouse was able to remain on the rotating rod before falling off was used to indicate motor function. Disease end point (or life span) was defined as either the loss of the righting reflex (inability to right the torso within 10 s) or a greater than 20% weight loss (14).

Western Blot—Spinal cords from P150 WT, $SOD1^{G93A}$, $snph^{-/-}$, and $SOD1^{G93A}$ /$snph^{-/-}$ mice were homogenized. 20 μg of homogenates were loaded and detected with monoclonal antibodies against hSOD1, cytochrome *c*, p115, and a polyclonal antibody against SNPH. Proteins were detected by ECL systems. Results were scanned and analyzed by Gel pro (Roper Industries).

Statistical Analysis—Statistical analyses of means for more than two groups were performed using one-way analysis of variance (ANOVA) with the categories of genotype and age as independent factors followed by the Tukey-Kramer post-hoc test for pair-wise comparisons. For analyses of means involving only two groups with a sample size $n < 30$, the F-test was used to determine if the variances between the two groups was significantly different. For samples with a significant difference in variance, the Welch's *t* test was applied. Student's *t* test was applied for the samples with an insignificant difference in variance or where $n \geq 30$. The null hypothesis was rejected at the 0.05 levels. Results for the mobility studies are expressed as the mean percentage of observed mitochondria in the mobile state ± S.E. Disease onset and lifespan are expressed as mean postnatal days ± S.D. All statistical computations were carried out using Prism (Graphpad Software).

[4] Animal care and use in this study were carried out in accordance with National Institutes of Health guidelines and was approved by the National Institutes of Health, NINDS/NIDCD Animal Care and Use Committee.

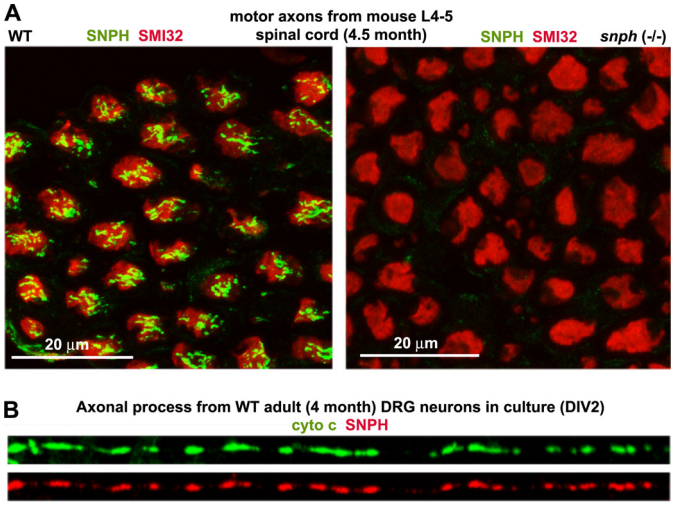

FIGURE 1. **SNPH is expressed in axons from spinal cord and targeted to axonal mitochondria in adult DRG neurons**. *A*, transverse sections of ventral roots (*axons*) from lumbar spinal cords of adult WT and *snph*$^{-/-}$ mice (P150) were co-stained with antibodies against SNPH (*green*) and neurofilaments (SMI32) (*red*). SNPH is localized within motor axon bundles from WT but not *snph*$^{-/-}$ mouse spinal cords. Scale bars: 20 μm. *B*, representative image showing co-localization of SNPH (*red*) and mitochondrial marker cytochrome *c* (*green*) in the axons of cultured DRG neurons from 4-month-old WT mice.

RESULTS

The SOD1^{G93A}/snph$^{-/-}$ Mice Exhibit Increased Axonal Mitochondrial Mobility—Our previous study demonstrated that SNPH, an axonal mitochondria-associated protein, serves as a docking receptor that specifically immobilizes axonal mitochondria. Deleting murine *snph* results in a dramatic increase in the percentage of axonal mitochondria in the mobile state (76 ± 20%) in cultured hippocampal neurons relative to wild-type controls (36 ± 15%) (12). To determine whether SNPH is also expressed in motor neuron axons, we immunostained transverse sections of motor axons sending out from the spinal cords of adult wild-type (WT) and *snph*$^{-/-}$ mice at postnatal day 150 (P150), and confirmed that SNPH is localized within motor axon bundles from WT but not *snph*$^{-/-}$ mouse spinal cords (Fig. 1*A*). SNPH targets to axonal mitochondria in cultured embryonic hippocampal neurons (12) and mature dorsal root ganglion (DRG) neurons isolated from adult mice (Fig. 1*B*). Thus, our *snph*$^{-/-}$ mice provide an ideal genetic tool to assess the role of increased mobility of axonal mitochondria in the pathogenesis of SOD1^{G93A} mice by generating crossed SOD1^{G93A}/*snph*$^{-/-}$ mice.

We first examined hSOD1 levels in spinal cord homogenates from adult (P150) mice of four genotypes: WT, SOD1^{G93A}, *snph*$^{-/-}$, and the crossed SOD1^{G93A}/*snph*$^{-/-}$ (Fig. 2*A*). No SNPH was detected in SOD1^{G93A}/*snph*$^{-/-}$ mice. Crossbreeding did not significantly alter hSOD1^{G93A} expression: normalized intensity of hSOD1 in SOD1^{G93A}/*snph*$^{-/-}$ mice was 90.25 ± 15.98% relative to that of SOD1^{G93A} mice ($p = 0.28$, $n = 9$ from 3 littermates).

To confirm that *snph* deletion resulted in increased axonal mitochondrial mobility in the crossed SOD1^{G93A}/*snph*$^{-/-}$ mice, we selected live DRG neurons from adult disease stage mice instead of embryonic motor neurons for time-lapse imaging analysis due to four critical factors. First, motor neuron degeneration and symptoms of ALS are progressive and age-dependent, thus it would be more clinically relevant to assess mitochondrial transport in neurons isolated from adult mice exhibiting disease symptoms rather than from embryos. Second, it is technically impossible to culture motor neurons from adult mice. Third, both motor neurons and DRG neurons show similar altered axonal transport in SOD1^{G93A} mice (16), thus DRG neurons from aged disease-stage mice have been widely used for study of defective axonal transport in the ALS-linked mouse models. Fourth, SNPH targets to axonal mitochondria in DRG neurons from adult mice (Fig. 1*B*), deleting *snph* substantially increases axonal mitochondrial mobility in cultured DRG neurons from adult mice relative to that from WT littermates (Fig. 2, *C* and *D*), providing an ideal live neuronal model to assess mitochondrial mobility.

We examined axonal mitochondrial mobility in live DRG neurons from four genotypes of age-matched adult mice (P120–125). Mitochondria were labeled at DIV2 with MitoTracker red CMX-Ros (100 nM for 20 s) (Fig. 2*B*), followed by time-lapse imaging. Kymographs were used to show the relative mobility of axonal mitochondria (Fig. 2*C*). Consistent with the axonal transport defects observed in embryonic motor neurons and adult DRG neurons (10, 11, 16), axonal mitochondria in SOD1^{G93A} DRG neurons showed reduced mobility (13.54 ± 0.38%, mean ± S.E.), anterograde transport (10.66 ± 0.77%), and retrograde transport (2.88 ± 0.46%) compared with age-matched WT DRG neurons (total mobility: 21.35 ± 1.08%, $p <$ 0.001; anterograde: 14.74 ± 1.05%, $p < 0.001$; retrograde: 6.61 ± 0.78%, $p < 0.001$) (Fig. 2*D*). In contrast, axonal mitochondria in both *snph*$^{-/-}$ and SOD1^{G93A}/*snph*$^{-/-}$ DRG neurons exhibited a statistically significant increase in total mobility (37.49 ± 1.74%, $p < 0.001$; 33.37 ± 1.22%, $p < 0.001$, respectively), anterograde transport (25.30 ± 1.16%, $p < 0.001$; 24.06 ± 1.20%, $p < 0.001$, respectively), and retrograde transport (12.18 ± 1.02%, $p < 0.001$; 9.31 ± 1.22%, $p < 0.001$, respectively) relative to WT DRG neurons (Fig. 2*D*, also see supplemental Movies S1–S4 available online). In addition, the axonal mitochondrial density in SOD1^{G93A} DRG neurons was also significantly reduced (Fig. 2*E*), which is consistent with a reduced axonal mitochondrial density observed in SOD1^{G93A} embryonic motor neurons (10). Interestingly, enhanced axonal mitochondrial mobility in SOD1^{G93A}/*snph*$^{-/-}$ mice rescued the deficit in mitochondrial density. Thus, the crossed SOD1^{G93A}/*snph*$^{-/-}$ mice provide a valuable model to assess the impact of increased (rescued) axonal mitochondrial mobility and density on motor neuron degeneration in ALS-linked mutant mice.

Both SOD1^{G93A} and Crossed SOD1^{G93A}/snph$^{-/-}$ Mice Display Similar ALS-like Disease Phenotypes—First, we evaluated the SOD1^{G93A} and SOD1^{G93A} /*snph*$^{-/-}$ phenotypes against WT and *snph*$^{-/-}$ controls using body weight and motor coordination parameters. We found that both SOD1^{G93A} and SOD1^{G93A} /*snph*$^{-/-}$ mice exhibited similar clinical evidence of motor neuron disease. By postnatal day 150 (P150), both genotypes had developed weakness accompanied by hind limb muscle wasting. When suspended by the tail, both SOD1^{G93A} and SOD1^{G93A} /*snph*$^{-/-}$ mice failed to extend their hind limbs (Fig. 3*A*). We weighed the animals and tested motor coordination monthly during the first 3 months of age and then weekly after

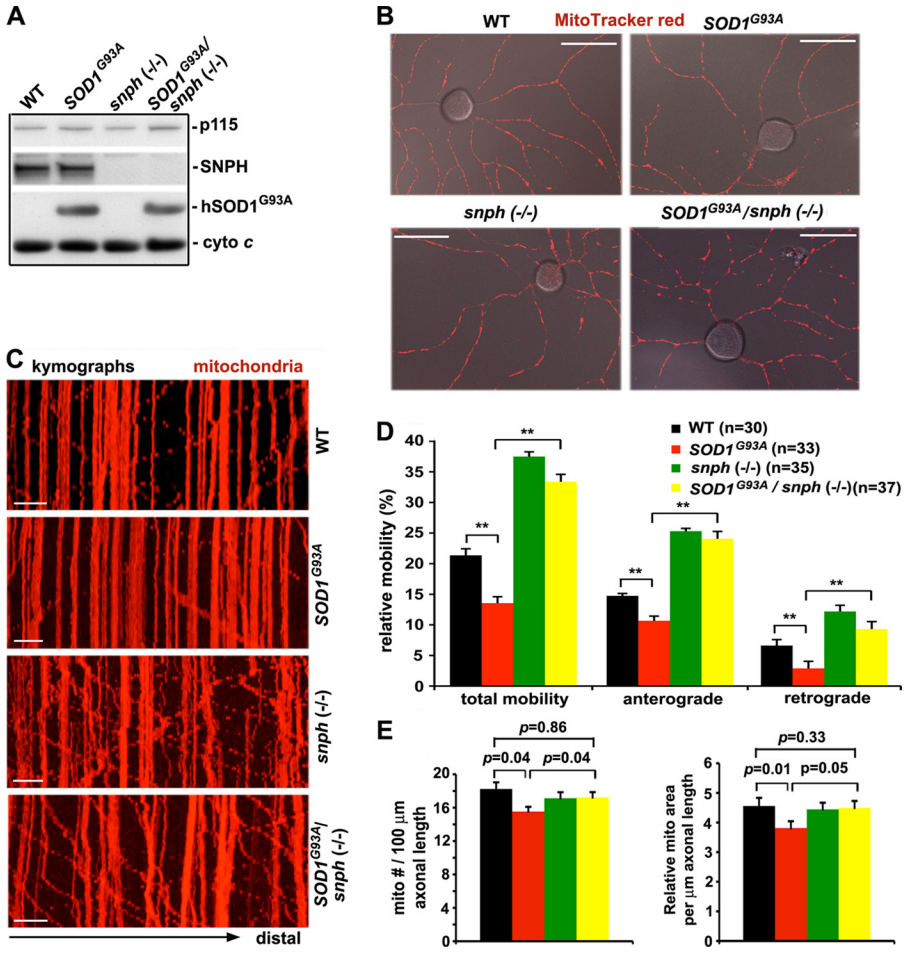

FIGURE 2. **Cultured DRG neurons from adult *snph*$^{-/-}$ and SOD1^{G93A}/*snph*$^{-/-}$ mice exhibit enhanced axonal mitochondrial mobility.** *A*, representative immunoblot showing SNPH and SOD1 expression in mice of four different genotypes. Equal amounts (20 mg) of spinal cord homogenate from P150 mice were sequentially blotted on the same membranes, which were stripped between each antibody application. Golgi marker p115 and mitochondrial marker cytochrome *c* serve as loading controls. The blots are representative of nine repeats from three pairs of littermates. *B*, representative DIV2 DRG neurons from adult mice labeled with MitoTracker red CMX-Ros. Scale bars: 50 μm. *C*, representative kymographs showing the relative mobility of axonal mitochondria in cultured DRG neurons (DIV2) from four genotypes of mice at ages between P120 and P125. *Vertical lines* represent stationary mitochondria and *oblique lines* or *curves* indicate mobile ones. The *arrow* in the bottom points toward distal axonal processes. Time-lapse sequences of 1,024 × 1,024 pixels (8 bits) were collected at ~10-s intervals for 50 images during 8.3 min. Scale bars: 10 μm. *D*, quantitative analysis of the percentage of total mobile axonal mitochondria and anterogradely *versus* retrogradely transported mitochondria. The number of DRG neurons examined for each genotype (from three littermates) is indicated in *parentheses*. Total axonal length measured was 4008.62 μm (WT), 4327.84 μm (*snph*$^{-/-}$), 4715.33 μm (SOD1^{G93A}), and 3744.38 μm (SOD1^{G93A}/*snph*$^{-/-}$). Error bars, S.E. **, $p < 0.001$. *E*, quantitative analysis of axonal mitochondrial density in cultured adult DRG neurons (*DIV2*). Relative mitochondrial density was measured in the distal axonal processes (at least >100 μm away from the soma) and is expressed as the number of mitochondria per 100 μm axonal length (*left*) and normalized relative mitochondrial area per μm axonal length (*right*). Total axonal length measured was 2016.90 μm (WT), 3049.27 μm (SOD1^{G93A}), 2096.23 μm (*snph*$^{-/-}$), and 2137.13 μm (SOD1^{G93A}/*snph*$^{-/-}$).

that. Both WT and *snph*$^{-/-}$ mice continue to grow with age, and although male mice were ~20% heavier than their female counterparts in both *snph*$^{-/-}$ and WT genotypes, *snph*$^{-/-}$ mice were slightly lighter than their WT littermates. In contrast, both male and female SOD1^{G93A} and SOD1^{G93A}/*snph*$^{-/-}$ mice began to lose weight at 17–18 weeks of age (Fig. 3*B*) and exhibited deterioration in motor function beginning at ~18 weeks of age (Fig. 3*C*). Rotarod tests did not detect any significant difference in motor coordination between SOD1^{G93A} and SOD1^{G93A}/*snph*$^{-/-}$ mice ($p = 0.21$, Student's *t* test). As a control, *snph*$^{-/-}$ mice kept alive throughout the duration of the experiment and did not display any signs of motor deterioration, further confirming that increased axonal mitochondrial mobility in *snph*$^{-/-}$ mice has no observable impact on motor neuron function.

Second, we compared the average onset of disease and lifespan. We did not find any significant difference between SOD1^{G93A} and SOD1^{G93A}/*snph*$^{-/-}$ mice. The average disease onset in female SOD1^{G93A} and SOD1^{G93A}/*snph*$^{-/-}$ mice was 127 ± 7 days (n = 10) and 126 ± 7 days (n = 10), respectively, *versus* 123 ± 5 days (n = 10) and 127 ± 7 days (n = 9) for male *SOD1*^{G93A} and SOD1^{G93A}/*snph*$^{-/-}$ mice, respectively (Fig. 3*D*). The average lifespan of C57BL6 mice carrying a high copy number of the human mutant SOD1^{G93A} allele was 152 days, females had an average lifespan of 152 ± 6 days (n = 12) and males lived 152 ± 4 days (n = 11). Deleting *snph* had no significant impact on lifespan; female SOD1^{G93A}/*snph*$^{-/-}$ mice lived 151 ± 4 days (n = 10) and males lived 156 ± 5 days (n = 10) (Fig. 3*E*). Overall, enhancing axonal mitochondria mobility by crossing *snph*$^{-/-}$ *and* SOD1^{G93A} mice did not affect disease onset, progression or lifespan.

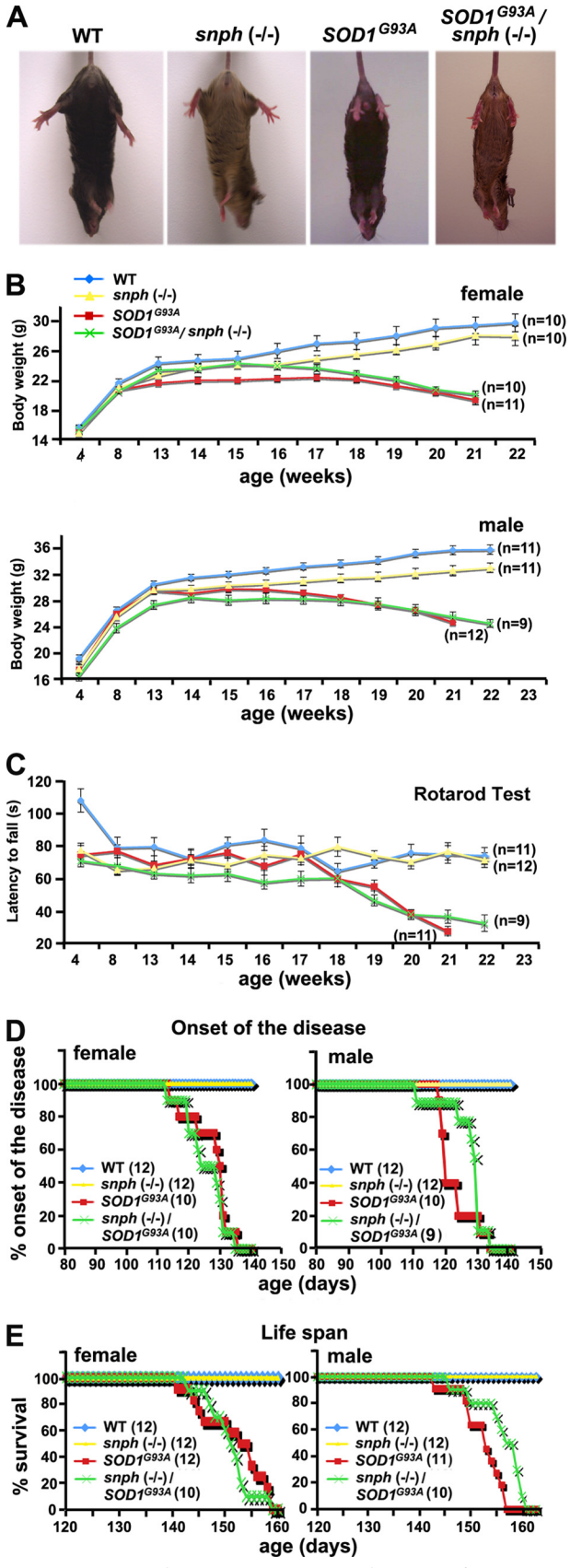

FIGURE 3. **Both SOD1^{G93A} and crossed SOD1^{G93A}/*snph*$^{-/-}$ mice display similar ALS-like disease phenotypes.** *A*, at P150, both SOD1^{G93A}, and SOD1^{G93A}/*snph*$^{-/-}$ mice fail to extend their hind limbs when suspended by their tail. The behavioral alteration is consistent across these two genotypes of mice. *B*, both SOD1^{G93A} and SOD1^{G93A}/*snph*$^{-/-}$ mice begin losing body weight at 17 weeks of age. Body weight of female (*upper*) and male (*lower*) mice was measured weekly. There was no significant difference in body mass between SOD1^{G93A} and SOD1^{G93A}/*snph*$^{-/-}$ mice at 21 weeks ($p = 0.33$ for female, $p = 0.39$ for male). *C*, both SOD1^{G93A} and SOD1^{G93A}/*snph*$^{-/-}$ mice exhibit similar deterioration in motor function beginning at 18 weeks as the disease progresses. Motor coordination was assessed weekly by the rotarod test. The apparatus was set to accelerate from 0 to 40 rpm over 180 s and the latency to fall was recorded. There was no significant difference in between SOD1^{G93A} and SOD1^{G93A}/*snph*$^{-/-}$ mice at age 21 weeks ($p = 0.12$). As a control, WT and *snph*$^{-/-}$ mice showed no signs of motor deterioration during the time frame of the experiment. *D* and *E*, enhanced axonal mitochondrial transport has no observable effect on the disease onset (*D*) and life span (*E*) of the crossed SOD1^{G93A}/*snph*$^{-/-}$ mice. The littermates of both SOD1^{G93A} and SOD1^{G93A}/*snph*$^{-/-}$ mice had similar disease onset, defined as the day following peak weight, and life span, defined as the loss of the righting reflex (loss of ability to right the torso after 10 s) or a >20% weight loss. The number of mice measured for each genotype is indicated in *parentheses*.

We next examined lumbar spinal cord motor neurons from P60 and P150 mice by labeling them with anti-SMI32 antibody (brown) and counterstaining with Nissl (purple). At the presymptomatic age (P60) (Fig. 4*A*, *upper two panels*), there was no significant difference in the spinal cord motor neuron count between WT and SOD1^{G93A} mice ($p = 0.06$) or between WT and SOD1^{G93A}/*snph*$^{-/-}$ mice ($p = 0.91$). When animals reached the end stage of the disease at about 150 days (Fig. 4*A*, *lower two panels*), there was a significant reduction in motor neuron number in both SOD1^{G93A} (54.90%, $p < 0.001$) and SOD1^{G93A}/*snph*$^{-/-}$ mice (55.88%, $p < 0.001$) compared with aged-matched WT and *snph*$^{-/-}$ mice (Fig. 4*B*).

As spinal cord and brain gliosis is a prominent feature in ALS (17, 18), next we immunostained GFAP (glial fibrillary acidic protein) and Iba-1 (ionized calcium binding adaptor molecule 1) to examine astrocytes and microglia, respectively. At 60 days of age, there was no significant difference in the normalized mean intensity of GFAP staining when SOD1^{G93A}/*snph*$^{-/-}$ and *snph*$^{-/-}$ mice were compared with WT mice (Fig. 5*A*). However, by P150 the normalized mean intensity of GFAP increased by 243.00 ± 23.45% in SOD1^{G93A} and by 201.51 ± 19.30% in SOD1^{G93A}/*snph*$^{-/-}$ mice compared with their WT littermates ($p < 0.001$). Interestingly, no significant difference in the mean intensity of GFAP was found between SOD1^{G93A} and SOD1^{G93A}/*snph*$^{-/-}$ mice ($p = 0.19$) (Fig. 5*B*). Consistently, we did not observe any difference in the normalized mean intensity of Iba-1 staining between any of the four genotypes at the presymptomatic age of 60 days (Fig. 5*C*). However, the normalized mean intensity of Iba-1 in the lateral ventral horn of P150 mice was significantly increased by 218.79 ± 18.80% in SOD1^{G93A} and by 175.06 ± 13,67% in SOD1^{G93A}/*snph*$^{-/-}$ mice compared with their WT littermates ($p < 0.001$). Again, there was no significant difference in the mean intensity of Iba-1 between SOD1^{G93A} and SOD1^{G93A}/*snph*$^{-/-}$ mice at their late disease stage ($p = 0.08$) or between the WT and *snph*$^{-/-}$ controls of the same age ($p = 0.50$) (Fig. 5*D*).

DISCUSSION

ALS is one of the most common motor neurodegenerative disorders. Whereas 90% of ALS cases are sporadic, 10% are familial, of which 20% are associated with mutations in SOD1 (7). Although the mechanisms underlying the selective degeneration of motor neurons in mutant SOD1 fALS remain elusive, the toxic mutant SOD1 gain of function is involved in the

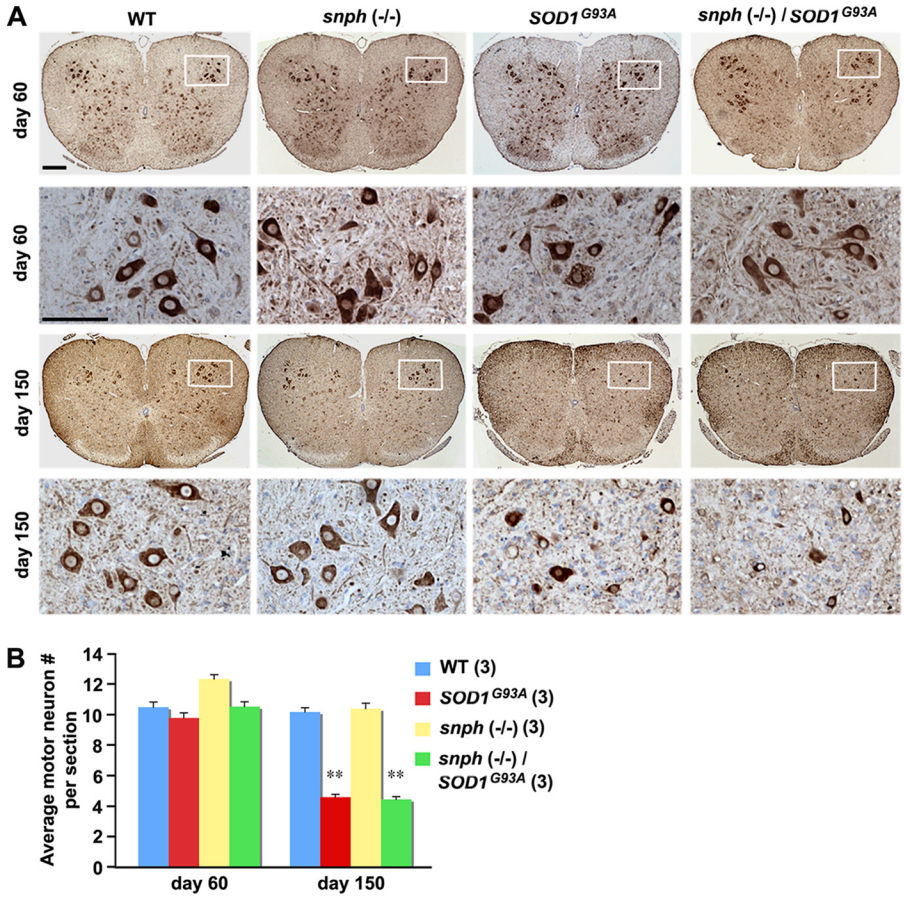

FIGURE 4. **Enhanced axonal mitochondrial transport does not prevent motor neuron loss in SOD1^{G93A}/*snph*$^{-/-}$ mice.** *A*, lumbar spinal cord motor neurons from P60 and P150 mice were labeled with anti-SMI32 antibody (*brown*) and counterstained with Nissl (*purple*). The second and fourth rows are high magnification images corresponding to the *boxed region* in each spinal cord section. Scale bars: 200 μm in low magnification and 100 μm in high magnification. *B*, average number of motor neurons per spinal cord section at P60 and P150. Note that at the presymptomatic age of 60 days, the spinal cord motor neuron count in SOD1^{G93A} and SOD1^{G93A}/*snph*$^{-/-}$ mice did not display any significant difference from the WT littermate ($p = 0.12$ for SOD1^{G93A}, $p = 0.91$ for SOD1^{G93A}/*snph*$^{-/-}$. In contrast, near the disease end stage (P150), a significant reduction in motor neuron count in both SOD1^{G93A} (54%, $p < 0.001$) and SOD1^{G93A}/*snph*$^{-/-}$ mice (55%, $p < 0.001$) was observed when compared with age-matched WT and *snph*$^{-/-}$ littermates. Three animals and a total of 90 spinal cord sections were examined for each genotype. Error bars: S.E. **, denote $p < 0.001$.

pathogenesis. Several hypotheses have been proposed, including the sequestration of essential cellular components in SOD1 aggregates (19), secretion of toxic factors by astrocytes expressing mutant SOD1 (20, 21), disruption of oxidative stress and calcium homeostasis, mitochondria-dependent apoptotic pathway (22), caspase-mediated apoptosis (23), and the ubiquitin-proteasome system (see reviews by 24, 25). Mutant human SOD1 accumulates in mitochondria of the brain, spinal cord, and motor neurons (26–28). Both morphological changes and dysfunction of axonal mitochondria have been observed in ALS patients and mutant SOD1 mouse models (15, 29–40).

There is also growing evidence that the perturbation and impairment of axonal transport (9, 14, 16, 41–47) is associated with the pathogenesis of ALS patients and mutant SOD1 mice. Mutant SOD1 has been shown to interact with both the anterograde kinesin-2 motor protein complex via kinesin-associated protein 3 (KAP3) (48), and the retrograde dynein-dynactin motor protein complex (49). Mitochondrial morphology and membrane dynamics, required for maintaining proper function, depend on proper mitochondrial mobility in neurons (50). Several studies have suggested that the onset of ALS symptoms is caused by alterations in mitochondrial transport induced by mutant SOD1 expression (10, 11). In the SOD1^{G93A} mouse model, disease onset and motor neuron death is immediately preceded by the accumulation of dysfunctional mitochondria in the distal region of the axon near the neuromuscular junction. However, whether altered mitochondrial transport plays a critical role in axonal degeneration or is merely a side effect of general defective axonal transport has not been addressed directly.

By genetically crossing *snph*$^{-/-}$ and SOD1^{G93A} mice, we provide the first genetic, cellular and pathological evidence that alteration of axonal mitochondrial mobility in SOD1^{G93A} mice plays a minor role in fALS-linked pathology. The deletion of *snph*, the docking receptor for axonal mitochondria, substantially increases the number of axonal mitochondria in the mobile state (12). We found that the lifespan and motor function of *snph*$^{-/-}$ mice dose not differ significantly from the C57BL/6 background WT mice used in our study despite a significant increase in mobile axonal mitochondria. This suggests that increasing axonal mitochondrial mobility by deleting *snph* does not adversely affect lifespan or motor function. Thus, crossing the SOD1^{G93A} transgenic mice with *snph* knock-out mice allowed us to directly investigate the role of mitochondrial

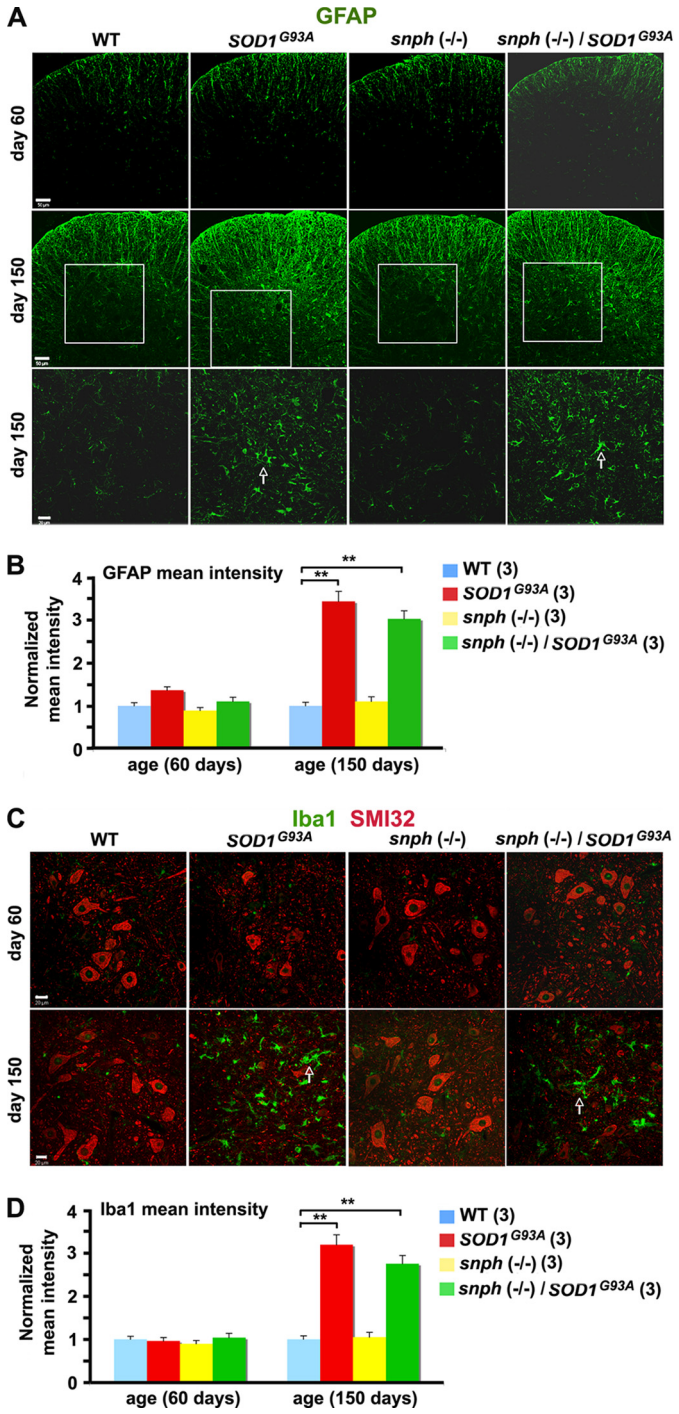

FIGURE 5. **Similar increased density pattern of astrocytes and microglia in the spinal cord of SOD1^{G93A} and SOD1^{G93A}/*snph*$^{-/-}$ mice.** *A*, increased GFAP staining in the lumbar spinal cord of SOD1^{G93A} and SOD1^{G93A}/*snph*$^{-/-}$ P150 mice indicates increased astrocyte density. The transverse sections of the lumbar region of the spinal cord derived from P60 or P150 mice were stained with an anti-GFAP antibody (*green*). The *boxed regions* in the second row are magnified and displayed in the third row of the panel. *Arrows* point to GFAP-labeled astrocytes. Scale bars: 50 μm at low magnification (rows 1 and 2) and 20 μm at high magnification (row 3). *B*, quantification of normalized GFAP mean intensity. *C*, increased microglia density (labeled with Iba1) and reduced motor neuron density (labeled with SMI32) in the spinal cord of SOD1^{G93A} and the crossed SOD1^{G93A}/*snph*$^{-/-}$ mice at P150. Transverse spinal cord sections were co-stained with antibodies against SMI32 (*red*) and Iba1 (*green*). *Arrows* indicate Iba1-labeled microglia. Scale bars: 20 μm. *D*, quantification of the normalized mean intensity of Iba-1. 9 slice sections from three mice for each genotype were examined. Error bars: S.E. ** denotes $p < 0.001$.

mobility in axonal degeneration by comparing clinical and histological observations of SOD1^{G93A} mice to SOD1^{G93A}/*snph*$^{-/-}$ mice. The crossed SOD1^{G93A}/*snph*$^{-/-}$ mice demonstrate significantly increased axonal mitochondrial mobility relative to SOD1^{G93A}. Additionally, both anterograde and retrograde transport was significantly increased in the SOD1^{G93A}/*snph*$^{-/-}$ mice, thus providing a unique model to directly assess the impact of increased axonal mitochondrial transport on motor neuron degeneration in the ALS-linked mutant mice.

Surprisingly, despite more than a 2-fold increase in axonal mitochondrial mobility in the crossed SOD1^{G93A}/*snph*$^{-/-}$ mice, we did not observe any clinical or histological difference in the disease course of this crossed mouse line compared with SOD1^{G93A} mice. Both SOD1^{G93A} and SOD1^{G93A}/*snph*$^{-/-}$ mice exhibited a similar weight loss pattern accompanied by deterioration of motor function beginning at ~17 weeks. Furthermore, both strains of mice exhibited 55% motor neuron loss and significant gliosis at the disease end stage. Our findings suggest that the role of mutant SOD1 in the pathogenesis of this ALS model is unlikely mediated through altering mitochondrial transport. The high mitochondrial mobility in both SOD1^{G93A}/*snph*$^{-/-}$ and *snph*$^{-/-}$ mice dose not correlate with lifespan or motor function, which further suggests that altered mitochondrial mobility probably plays a minor role in the pathogenesis of this mouse model.

We previously demonstrated that *snph*$^{-/-}$ embryonic hippocampal neurons have a slightly lower mitochondrial density than WT mice (12). In the present study, we did not observe a statistical difference in mitochondrial density in the distal axonal processes between adult *snph*$^{-/-}$ and WT mice. This may be attributable to developmental regulation of axonal mitochondrial transport. It was reported that mitochondria are more mobile in young neurons relative to mature neurons (51). Deleting *snph* in mice results in a more robust increase in axonal mitochondrial mobility of embryonic hippocampal neurons (76 ± 20%) relative to that of adult DRG neurons (37.49 ± 1.74%). Such a large increase in mobile mitochondria in embryonic neurons may impact their density in axons.

In contrast, there was a lower mitochondrial density in axons of SOD1^{G93A} DRG neurons relative to WT neurons. Deleting *snph* (SOD1^{G93A}/*snph*$^{-/-}$) rescued the deficit. Given the fact that the SOD1^{G93A}/*snph*$^{-/-}$ phenotype was clinically similar to the uncrossed SOD1^{G93A} phenotype, the reduced axonal mitochondrial density observed in SOD1^{G93A} mice does not critically contribute to the pathogenesis of fALS. It is likely that other factors including, but not limited to, protein aggregation and mitochondrial dysfunction caused by mutant SOD1 play a more significant role in the disease process. It is important to note that while many studies related to mitochondrial transport in ALS mice models have been carried out using the *SOD1*^{G93A} mutant, the disease process in this strain progresses rapidly with an average lifespan of 152 days. With such a short lifespan, we cannot exclude the possibility that the crossed SOD1^{G93A}/*snph*$^{-/-}$ mice do not live long enough for the genetic rescue to occur.

Our study suggests that the impairment of mitochondrial transport seen in SOD1^{G93A} mice may be a secondary effect of a more general alteration of axonal transport caused by mutant

aggregates or motor protein defects. In SOD1^{G93A} mice, a specific mutation in the dynein heavy chain produces a complete recovery of the axonal retrograde transport defect and rescues the phenotype (14). A *Cra1* mutation in *Dnchc1* improves the phenotype of SOD1^{G93A} mice and prolongs their survival period (52). Recent findings that the SOD1-dependent pathogenic mechanism impairs axonal transport in both familial and sporadic ALS indicate a general transport defect associated with ALS-linked neurodegeneration (46). Alterations of other transport cargos may play a more important role than defective mitochondrial transport. A shift in retrograde transport from survival-promoting to death-promoting signaling may be responsible for the rapid onset of symptoms in the SOD1^{G93A} mouse model (16). Misfolded mutant SOD1 associates with the outer membrane of mitochondria in spinal cord and motor neurons (26, 28) and damages mitochondrial membrane conductance and metabolites by directly binding to the voltage-dependent anion channel (VDAC) (40). Thus, mitochondria dysfunction, rather than impaired mobility, may be more important in rapid-onset motor neuron degeneration.

Acknowledgments—We thank X. Lin and Huaibin Cai (NIA, NIH) for generous help in training us in mouse pathology analysis and behavioral tests, and insightful discussion on the ALS mouse model. We also thank the following people: Q. Cai, Y. Chen, Y. Xie, R. Chia, K. Tsubota, and other members of the Sheng laboratory for technical help and critical comments; J. Tokita and M. Davis for editing the manuscript.

REFERENCES

1. Hollenbeck, P. J., and Saxton, W. M. (2005) *J. Cell Sci.* **118,** 5411–5419
2. Cai, Q., and Sheng, Z. H. (2009) *Neuron* **61,** 493–496
3. Macaskill, A. F., Rinholm, J. E., Twelvetrees, A. E., Arancibia-Carcamo, I. L., Muir, J., Fransson, A., Aspenstrom, P., Attwell, D., and Kittler, J. T. (2009) *Neuron* **61,** 541–555
4. Wang, X., and Schwarz, T. L. (2009) *Cell* **136,** 163–174
5. Hirokawa, N., Niwa, S., and Tanaka, Y. (2010) *Neuron* **68,** 610–638
6. Cleveland, D. W., and Rothstein, J. D. (2001) *Nat. Rev. Neurosci.* **2,** 806–819
7. Rosen, D. R., Siddique, T., Patterson, D., Figlewicz, D. A., Sapp, P., Hentati, A., Donaldson, D., Goto, J., O'Regan, J. P., and Deng, H. X. (1993) *Nature* **362,** 59–62
8. Gurney, M. E., Pu, H., Chiu, A. Y., Dal Canto, M. C., Polchow, C. Y., Alexander, D. D., Caliendo, J., Hentati, A., Kwon, Y. W., and Deng, H. X. (1994) *Science* **264,** 1772–1775
9. Sasaki, S., and Iwata, M. (1996) *Neurology* **47,** 535–540
10. De Vos, K. J., Chapman, A. L., Tennant, M. E., Manser, C., Tudor, E. L., Lau, K. F., Brownlees, J., Ackerley, S., Shaw, P. J., McLoughlin, D. M., Shaw, C. E., Leigh, P. N., Miller, C. C., and Grierson, A. J. (2007) *Hum. Mol. Genet.* **16,** 2720–2728
11. Magrané, J., Hervias, I., Henning, M. S., Damiano, M., Kawamata, H., and Manfredi, G. (2009) *Hum. Mol. Genet.* **18,** 4552–4564
12. Kang, J. S., Tian, J. H., Pan, P. Y., Zald, P., Li, C., Deng, C., and Sheng, Z. H. (2008) *Cell* **132,** 137–148
13. Ilieva, H. S., Yamanaka, K., Malkmus, S., Kakinohana, O., Yaksh, T., Marsala, M., and Cleveland, D. W. (2008) *Proc. Natl. Acad. Sci. U.S.A.* **105,** 12599–12604
14. Kieran, D., Hafezparast, M., Bohnert, S., Dick, J. R., Martin, J., Schiavo, G., Fisher, E. M., and Greensmith, L. (2005) *J. Cell Biol.* **169,** 561–567
15. Kong, J., and Xu, Z. (1998) *J. Neurosci.* **18,** 3241–3250
16. Perlson, E., Jeong, G. B., Ross, J. L., Dixit, R., Wallace, K. E., Kalb, R. G., and Holzbaur, E. L. (2009) *J. Neurosci.* **29,** 9903–9917
17. Boillée, S., Yamanaka, K., Lobsiger, C. S., Copeland, N. G., Jenkins, N. A., Kassiotis, G., Kollias, G., and Cleveland, D. W. (2006) *Science* **312,** 1389–1392
18. Yamanaka, K., Chun, S. J., Boillee, S., Fujimori-Tonou, N., Yamashita, H., Gutmann, D. H., Takahashi, R., Misawa, H., and Cleveland, D. W. (2008) *Nat. Neurosci.* **11,** 251–253
19. Bruijn, L. I., Houseweart, M. K., Kato, S., Anderson, K. L., Anderson, S. D., Ohama, E., Reaume, A. G., Scott, R. W., and Cleveland, D. W. (1998) *Science* **281,** 1851–1854
20. Clement, A. M., Nguyen, M. D., Roberts, E. A., Garcia, M. L., Boillée, S., Rule, M., McMahon, A. P., Doucette, W., Siwek, D., Ferrante, R. J., Brown, R. H., Jr., Julien, J. P., Goldstein, L. S., and Cleveland, D. W. (2003) *Science* **302,** 113–117
21. Nagai, M., Re, D. B., Nagata, T., Chalazonitis, A., Jessell, T. M., Wichterle, H., and Przedborski, S. (2007) *Nat. Neurosci.* **10,** 615–622
22. Guégan, C., Vila, M., Rosoklija, G., Hays, A. P., and Przedborski, S. (2001) *J. Neurosci.* **21,** 6569–6576
23. Li, M., Ona, V. O., Guégan, C., Chen, M., Jackson-Lewis, V., Andrews, L. J., Olszewski, A. J., Stieg, P. E., Lee, J. P., Przedborski, S., and Friedlander, R. M. (2000) *Science* **288,** 335–339
24. Bruijn, L. I., Miller, T. M., and Cleveland, D. W. (2004) *Annu. Rev. Neurosci.* **27,** 723–749
25. Pasinelli, P., and Brown, R. H. (2006) *Nat. Rev. Neurosci.* **7,** 710–723
26. Liu, J., Lillo, C., Jonsson, P. A., Vande Velde, C., Ward, C. M., Miller, T. M., Subramaniam, J. R., Rothstein, J. D., Marklund, S., Andersen, P. M., Bränström, T., Gredal, O., Wong, P. C., Williams, D. S., and Cleveland, D. W. (2004) *Neuron* **43,** 5–17
27. Vijayvergiya, C., Beal, M. F., Buck, J., and Manfredi, G. (2005) *J. Neurosci.* **25,** 2463–2470
28. Vande Velde, C., Miller, T. M., Cashman, N. R., and Cleveland, D. W. (2008) *Proc. Natl. Acad. Sci. U.S.A.* **105,** 4022–4027
29. Dal Canto, M. C., and Gurney, M. E. (1994) *Am. J. Pathol.* **145,** 1271–1279
30. Wong, P. C., Pardo, C. A., Borchelt, D. R., Lee, M. K., Copeland, N. G., Jenkins, N. A., Sisodia, S. S., Cleveland, D. W., and Price, D. L. (1995) *Neuron* **14,** 1105–1116
31. Vielhaber, S., Winkler, K., Kirches, E., Kunz, D., Büchner, M., Feistner, H., Elger, C. E., Ludolph, A. C., Riepe, M. W., and Kunz, W. S. (1999) *J. Neurol. Sci.* **169,** 133–139
32. Echaniz-Laguna, A., Zoll, J., Ribera, F., Tranchant, C., Warter, J. M., Lonsdorfer, J., and Lampert, E. (2002) *Ann. Neurol.* **52,** 623–627
33. Mattiazzi, M., D'Aurelio, M., Gajewski, C. D., Martushova, K., Kiaei, M., Beal, M. F., and Manfredi, G. (2002) *J. Biol. Chem.* **277,** 29626–29633
34. Wiedemann, F. R., Manfredi, G., Mawrin, C., Beal, M. F., and Schon, E. A. (2002) *J. Neurochem.* **80,** 616–625
35. Dupuis, L., di Scala, F., Rene, F., de Tapia, M., Oudart, H., Pradat, P. F., Meininger, V., and Loeffler, J. P. (2003) *FASEB J.* **17,** 2091–2093
36. Higgins, C. M., Jung, C., and Xu, Z. (2003) *BMC Neurosci.* **4,** 16
37. Damiano, M., Starkov, A. A., Petri, S., Kipiani, K., Kiaei, M., Mattiazzi, M., Flint, B. M., and Manfredi, G. (2006) *J. Neurochem.* **96,** 1349–1361
38. Sasaki, S., and Iwata, M. (2007) *J. Neuropathol. Exp. Neurol.* **66,** 10–16
39. Nguyen, K. T., García-Chacón, L. E., Barrett, J. N., Barrett, E. F., and David, G. (2009) *Proc. Natl. Acad. Sci. U.S.A.* **106,** 2007–2011
40. Israelson, A., Arbel, N., Da Cruz, S., Ilieva, H., Yamanaka, K., Shoshan-Barmatz, V., and Cleveland, D. W. (2010) *Neuron* **67,** 575–587
41. Warita, H., Itoyama, Y., and Abe, K. (1999) *Brain. Res.* **819,** 120–131
42. Williamson, T. L., and Cleveland, D. W. (1999) *Nat. Neurosci.* **2,** 50–56
43. Hafezparast, M., Klocke, R., Ruhrberg, C., Marquardt, A., Ahmad-Annuar, A., Bowen, S., Lalli, G., Witherden, A. S., Hummerich, H., Nicholson, S., Morgan, P. J., Oozageer, R., Priestley, J. V., Averill, S., King, V. R., Ball, S., Peters, J., Toda, T., Yamamoto, A., Hiraoka, Y., Augustin, M., Korthaus, D., Wattler, S., Wabnitz, P., Dickneite, C., Lampel, S., Boehme, F., Peraus, G., Popp, A., Rudelius, M., Schlegel, J., Fuchs, H., Hrabe de Angelis, M., Schiavo, G., Shima, D. T., Russ, A. P., Stumm, G., Martin, J. E., and Fisher, E. M. (2003) *Science* **300,** 808–812
44. Ligon, L. A., LaMonte, B. H., Wallace, K. E., Weber, N., Kalb, R. G., and Holzbaur, E. L. (2005) *Neuroreport* **16,** 533–536
45. Morfini, G. A., Burns, M., Binder, L. I., Kanaan, N. M., LaPointe, N., Bosco, D. A., Brown, R. H., Jr., Brown, H., Tiwari, A., Hayward, L., Edgar, J., Nave,

K. A., Garberrn, J., Atagi, Y., Song, Y., Pigino, G., and Brady, S. T. (2009) *J. Neurosci.* **29,** 12776–12786
46. Bosco, D. A., Morfini, G., Karabacak, N. M., Song, Y., Gros-Louis, F., Pasinelli, P., Goolsby, H., Fontaine, B. A., Lemay, N., McKenna-Yasek, D., Frosch, M. P., Agar, J. N., Julien, J. P., Brady, S. T., and Brown, R. H., Jr. (2010) *Nature Neurosci.* **13,** 1396–1405
47. Guipponi, M., Li, Q. X., Hyde, L., Beissbarth, T., Smyth, G. K., Masters, C. L., and Scott, H. S. (2010) *J. Mol. Neurosci.* **41,** 172–182
48. Tateno, M., Kato, S., Sakurai, T., Nukina, N., Takahashi, R., and Araki, T. (2009) *Hum. Mol. Genet.* **18,** 942–955
49. Zhang, F., Ström, A. L., Fukada, K., Lee, S., Hayward, L. J., and Zhu, H. (2007) *J. Biol. Chem.* **282,** 16691–16699
50. Chen, H., and Chan, D. C. (2009) *Hum. Mol. Genet.* **18,** 169–176
51. Chang, D. T., and Reynolds, I. J. (2006) *Neuroscience* **141,** 727–736
52. Teuchert, M., Fischer, D., Schwalenstoecker, B., Habisch, H. J., Böckers, T. M., and Ludolph, A. C. (2006) *Exp. Neurol.* **198,** 271–274